

A NEW PERSPECTIVE ON MOND

D.V. BUGG ¹

Department of Physics, Queen Mary, University of London, London E1 4NS, UK

Abstract

A novel interpretation of MOND is presented. For galactic data, in addition to Newtonian acceleration, there is an attractive acceleration peaking at Milgrom's parameter a_0 . The peak lies within experimental error where $a_0 = cH_0/2\pi$; H_0 is the present-time value of the Hubble constant and c the velocity of light. The physical interpretation of this relation and its connection to Dark Energy are discussed.

PACS numbers: 04.50.Kd, 98.62.Dm

1 Introduction

It has long been known that rotation curves of galaxies disagree with Newton's law. Famaey and McGaugh have recently provided a review of all aspects of the data, with an exhaustive list of references [1]. The most relevant astrophysical data will be discussed here.

In 1983, Milgrom proposed a modification of Newtonian mechanics called MOND (Modified Newtonian Dynamics) [2], [3]. This has three distinct features. Firstly, the observed total acceleration a depends on the Newtonian acceleration g_N as

$$a = g_N / \mu(\chi); \quad (1)$$

μ is an empirical smooth function of $\chi = a/a_0$; a_0 is a universal constant $\sim 1.2 \times 10^{-10} \text{ m s}^{-2}$ for all galaxies. The second feature is that for vanishingly small g_N ,

$$a \rightarrow \sqrt{a_0 g_N}. \quad (2)$$

Thirdly, galactic dynamics are invariant under scaling of time and space for very low g_N :

$$(t, \mathbf{r}) \rightarrow \lambda(t, \mathbf{r}), \quad (3)$$

where λ is a scaling factor [4]. A star with rotational velocity v in equilibrium with centrifugal force satisfies

$$v^2/r = \sqrt{\frac{a_0 G M}{r^2}}; \quad (4)$$

G is the gravitational constant and M the galactic mass within radius r ; so r cancels and

$$v^4 = a_0 G M. \quad (5)$$

This agrees well with the empirical Tully-Fisher relation between observed velocities at the edges of galaxies and their luminosities [5]. McGaugh showed that this relation applies over > 5 decades of galactic masses from 10^6 to $\sim 10^{12} M_\odot$ after including the mass of gas and dust in

¹email: david.bugg@stfc.ac.uk

each galaxy [6]. It is important that in MOND there is only one free parameter a_0 , fitted to all galaxies once a particular form for $\mu(x)$ has been chosen.

In the Λ CDM cosmological model, the parameter a_0 does not appear. There are three recent papers pointing out that a shift of paradigm is required to describe the data more precisely [7], [8], [9]. Kroupa et al. and Famaey et al. discuss simulations based on the standard cosmological model Λ CDM. They both point out the prediction that the main Dark Matter halo hosting a large galaxy like the Milky Way should produce 100–600 roughly isotropic sub-halos. However, the Milky Way has only 24 satellites (and Andromeda ~ 28 [10]) which are highly correlated in both radial and momentum phase space. They lie mostly within rotationally supported thin discs. This has been strongly confirmed by Ibata et al. [11]. These authors all conclude that Λ CDM is at best incomplete and misses essential physics. There is a further interesting paper of Lüghausen et al. concerning a polar ring galaxy [12]. This galaxy has a small bright gas-poor disc with a large central bulge, but in addition an orthogonal gas-rich disc, referred to as a polar ring. They show that the observed velocities in both discs are well predicted by MOND.

Another Λ CDM prediction is that dwarf galaxies formed from tidal material during galaxy encounters cannot contain substantial amounts of Dark Matter; MOND fits them well. McGaugh and Milgrom [9] make an important comment that tidal effects of large galaxies on their satellite galaxies must be taken into account in drawing conclusions about the satellites. The objective of the present paper is to search for an explanation of the observed discrepancies.

The conventional Λ CDM paradigm is that Dark Matter condenses gravitationally and then galaxies form inside this condensate. This is a two-step process. The procedure adopted here is to use commonly used forms of Milgrom's μ function to determine the non-Newtonian component of the acceleration observed at the edges of galaxies; it peaks at or close to a_0 where it is bigger than g_N by a large factor ~ 171 . This acceleration is then integrated to determine the associated energy function. The result fits naturally to a Fermi function with the same negative sign as that of gravity. The Fermi function lowers the total energy by $0.5 GM$ at radius r_0 where g_N reaches a_0 ; here M is the mass within radius r_0 . This Fermi function takes the same form as the energy gap observed in doped semiconductors. It is adopted as the effective Hamiltonian for the non-Newtonian interaction. It is interpreted as evidence that a Fermi-Dirac condensate forms in the graviton-nucleon interaction (not the gravitational interaction itself) near radius r_0 . There are then four further clues which fit like a glove to the existence of this condensate. One is that $2\pi a_0 = cH_0$ within experimental errors; here c is the velocity of light and H_0 is the local value of the Hubble acceleration. This results in a direct relation between a_0 and Dark Energy. Dark Matter is no longer needed in this one-step process.

Most discussions of galactic rotation curves use the asymptotic form of the acceleration. Here attention is focussed on accelerations close to a_0 , between $\sim 10^{-8}$ and $\sim 10^{-12}$ m s $^{-2}$.

An independent observation of the role of a_0 has appeared in globular clusters within the last few years. These spherical clusters of stars have dimensions of a few parsec (pc), i.e. a factor $\sim 10^4$ smaller than the Milky Way. They are believed to be the remnants of dwarf galaxies, some old and some quite young. Scarpa et al. reported initially on two globular clusters situated 16–19 kpc from the Milky Way [13]. The equilibrium of such clusters is controlled by Jeans' Law. Scarpa et al. traced the velocity dispersion of 184 stars at large radius, identified as being members of one globular cluster (rather than interlopers), and 146 stars in the second cluster. The velocity dispersion is maximal at the centre of each cluster. They traced it to a radius twice that where g_N reaches a_0 . Velocity dispersions deviate rather abruptly from g_N as it decreases

through a_0 . Tidal heating by the Milky Way varies as r^{-3} , and is at least one order of magnitude smaller, making its effect negligible.

Scarpa et al. have made observations of a further 6 globular clusters. Hernandez and Jiménez give the algebra relating velocity dispersions of stars to Newtonian acceleration using Jeans' Law [14]. Hernandez, Jiménez and Allen report a detailed study of the velocity dispersion profiles of all 8 globular clusters [15]. Like Scarpa et al., they conclude that tidal effects are significant only at radii larger by factors 2–10 than the radius where MOND flattens the curves. They also show that the velocity dispersion σ varies with the mass M of the cluster as M^{-4} within errors; this is the expected analogue of the Tully-Fisher relation arising from Jeans' Law. This result is independent of luminosity measurements used in interpreting galactic rotation curves. In galaxies, the mass M within a particular radius is not easy to determine, and is usually taken as the mass where rotation curves flatten out. Further study of globular clusters is desirable.

Differences between the μ functions used for MOND are illustrated in Fig. 19 of the review of Famaey and McGaugh [1]. The smoothest form, given by Milgrom [16], is used here:

$$\mu(\chi) = \sqrt{1 + 1/(4\chi^2)} - 1/(2\chi). \quad (6)$$

The algebraic form with which globular clusters are fitted is closely consistent with this equation.

The layout of this paper is as follows. Section 2 presents in Fig. 1(a) the observed acceleration on the logarithmic scale of g_N adopted by Milgrom [16]; it gives the algebra for the chosen form of $\mu(x)$, where $x = \log_{10} g_N$. From this, the difference between the observed acceleration and g_N is derived and shown in Fig. 1(b). This is then integrated to find its associated energy function $W(x)$, Fig. 1(c). I follow the convention that the zero of the Newtonian potential is taken locally, ignoring the effects of Dark Energy over the Universe as a whole. The height of the Fermi function may be interpreted as an energy gap.

There is further evidence of quantum mechanics at work. The asymptotic form of the total acceleration can likewise be integrated. In Section 3, this is shown to lead to a weak logarithmic tail to the Newtonian potential. The interpretation is that quantum mechanical mixing between the Newtonian potential and the asymptotic form allows the wavelength of gravitons trapped in the Newtonian potential to expand. This lowers the zero-point energy.

These two indications of quantum effects should not be surprising. Hawking has demonstrated that Quantum Mechanics plays an important role in the physics of Black Holes [17], where the acceleration is very large. A standard Particle Physics result is that the graviton-nucleon interaction should obey a dispersion relation as a function of the amplitude of g_N (with a non-analytic logarithmic term in addition). Gravitons with a wavelength of galactic dimensions are at the extreme infra-red end of the spectrum. With such a wavelength, a single graviton interacts coherently with nucleons over complete clusters of stars.

Section 3 examines the idea that there is quantum mechanical mixing between g_N and the Hubble acceleration. This mixing is a well known effect in Particle Spectroscopy for two eigenfunctions having different basis states. The standard treatment is to use the Bogoliubov-Valatin transformation [18] [19], which leads to the Breit-Rabi equation for the mixing.

Section 4 relates the observed asymptotic acceleration to Dark Energy and a subtle connection with the Hubble acceleration. Subsection 4.1 then draws an analogy with Condensed Matter Physics and the well understood Symmetry Breaking in Particle Physics. Section 5 makes extensive comments on avenues for further work and Section 6 summarises conclusion.

2 THE MODEL NEAR a_0

From equation (6),

$$\mu = g_N/a = \sqrt{1 + \frac{a_0^2}{4a^2}} - \frac{a_0}{2a} \quad (7)$$

$$(g_N/a + a_0/2a)^2 = 1 + (a_0/2a)^2 \quad (8)$$

$$g_N^2 + a_0 g_N = a^2. \quad (9)$$

The cancellation of the two terms $a_0/2a^2$ is typical of a dispersion relation and emerges as an important point in Section 3.

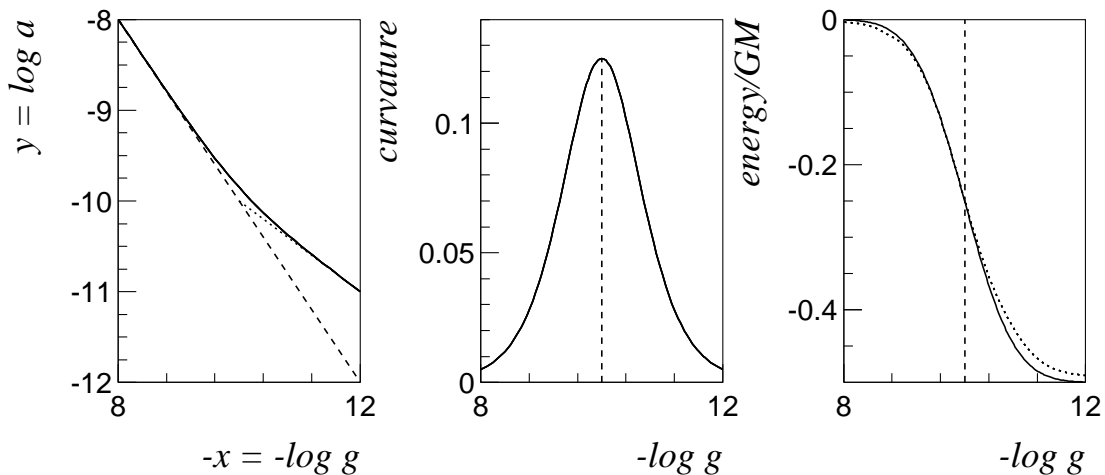


Figure 1: (a) The full curve shows the result of equation (10); the dashed line shows g_N , and the dotted one a straight line given by $\sqrt{a_0 g_N}$; (b) the peak arising from curvature of the full curve in (a); (c) full curve: the energy derived from (b); the dashed curve is discussed in Section 3; vertical dashed lines mark a_0 .

Milgrom plots the log of total acceleration against the log of gravitational acceleration for systems of different masses [20]. It is inconvenient to use axes to the base 10, so they will be replaced in the algebra which follows by conversion to \ln_e . From Eq. (9)

$$y = \ln_e \sqrt{g_N^2 + a_0 g_N}; \quad (10)$$

$$x = \ln_e g_N. \quad (11)$$

From equation (10),

$$e^{2y} = e^{2x} + a_0 e^x \quad (12)$$

$$dy/dx = (e^x + a_0/2)(e^x + a_0)^{-1} \quad (13)$$

$$d^2y/dx^2 = (a_0/2)e^x(e^x + a_0)^{-2} \quad (14)$$

$$d^3y/dx^3 = (a_0/2)e^x(a_0 - e^x)/(e^x + a_0)^{-3}; \quad (15)$$

d^3y/dx^3 goes to zero at $g = a_0$. [There are higher order terms too.] The curvature d^2y/dx^2 has a maximum value at $x = a_0$, where $d^2y/dx^2 = 1/8$.

In galaxies, perturbations arise from thermal and pressure effects. Some narrow structures are observed in rotation curves, for example from bars in large galaxies. These may be fitted empirically using Poisson's equation for mass structures appearing in the gravitational potential. The MOND component 'rides' such structures smoothly, see Figs. 21 and 29 of Famaey and McGaugh [1]. An immediate question is why Planck's constant does not appear in results for galactic rotation curves. The reason is that galaxies are noisy enough to hide it.

Using $a_0 = cH_0/2\pi$, the maximum curvature is expected at $a_0 = (1.113 \pm 0.046) \times 10^{-10} \text{ m s}^{-2}$, i.e. $\log_{10} a_0 = -9.953$. McGaugh summarises a large number of papers comparing the Tully-Fisher relation with models of galaxy formation [21]. He concludes that gas rich galaxies give the best determination of the baryonic masses of galaxies: $a_0 = (1.3 \pm 0.3) \times 10^{-10} \text{ m s}^{-2}$. A slightly lower value $1.22 \pm 0.33 \times 10^{-10} \text{ m s}^{-2}$ is found by Gentile, Famaey and de Blok [22]. Fig. 1(b) shows d^2y/dx^2 as a peak dW/dx in the acceleration at a_0 , marked by the dashed line; here W is the energy of the 'extra' contribution. Results are insensitive to the precise value of a_0 , so figures and arithmetic are simplified by setting $a_0 = 10^{-10} \text{ m s}^{-2}$. The full curve is well approximated by a Gaussian for the acceleration:

$$d^2y/dx^2 = 0.125 \exp -[\gamma(x - a_0)^2] \quad (16)$$

with $\gamma = 1.175$, i.e. the Gaussian drops to half-height at 9.6% of the value of x at the peak in Fig. 1(b). The conclusion is that galaxies have considerable stability.

2.1 Alternative forms for μ

Other forms for $\mu(\chi)$ have been used to fit galactic rotation curves. Two common examples are (A) $\mu(\chi) = \chi/(1 + \chi)$, (B) $\chi/\sqrt{1 + \chi^2}$. Both forms have the effect of moving the peak of the curvature slightly: from $x = -10$ to -9.7 for A and to -9.85 for B. The height of the peak for A is scaled by a factor 0.78 and the curve becomes correspondingly wider, resulting in a tail reaching 0.012 at $x = -8.2$ and -11.8 . The result for Fig. 1(c) is that the top of the Fermi function is 4% of GM lower, and the bottom of the curve higher by the same amount, but the central part of the Fermi function is unchanged and still centred very close to $x = -10$. Form B produces the converse effect: a higher, narrower peak in Fig. 1(b) and a Fermi function beginning closer to the top and finishing closer to the bottom of Fig. 1(c), but with its central section undisturbed.

A detail is that one might consider the possibility that the smooth curve of Fig. 1(a) could be derived from the dashed and dotted lines. This would give rise to a sharp cusp in Fig. 1(b). Such cusps are known in Particle Physics, but arise only at the opening of phase space for a new reaction channel [23]. However, no such threshold exists in galactic phenomena.

In Fig. 1(a), the dashed line corresponding to g_N intersects at $x = -10$ with the straight line fitted to $\sqrt{a_0 g_N}$. This suggests that there is a cross-over between two eigenfunctions corresponding to two asymptotic regimes. This is a familiar result in Particle Physics. Historically, it was first observed in variations of atomic energy levels in a magnetic field. It arises there from differences in magnetic moments for different levels, some of which share one component. The result for that case is sketched in Fig. 2. The two dashed lines show the variation of energy eigenstates with magnetic field.

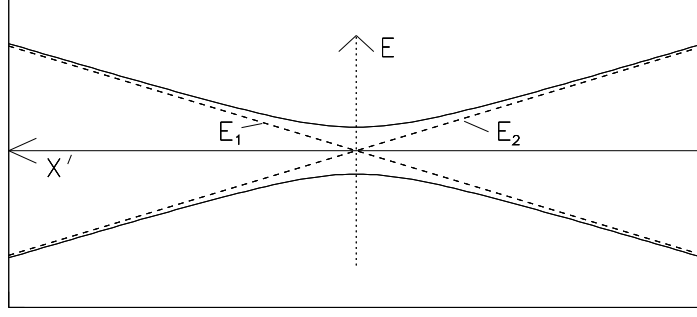


Figure 2: Sketch of two crossing atomic lines; full lines show them including mixing, dashed lines without; E_1 and E_2 label the convention for eigenvalues in the case of no mixing.

For the two mixed states,

$$H_{11}\Psi_1 + V\Psi_2 = E\Psi_1 \quad (17)$$

$$H_{22}\Psi_2 + V\Psi_1 = E\Psi_2. \quad (18)$$

where V is the mixing Hamiltonian. The solution of these coupled equations is

$$(H_{11} - E)(H_{22} - E) - V^2 = 0. \quad (19)$$

This equation was first derived in 1931 by Breit and Rabi [24]. The same formalism describes mixing between the three neutrinos ν_e , ν_μ and ν_τ and also the CKM matrix of QCD. For galaxies, classical expectation values $\langle H_{11} \rangle$ and $\langle H_{22} \rangle$ are to be substituted into Eq. (19).

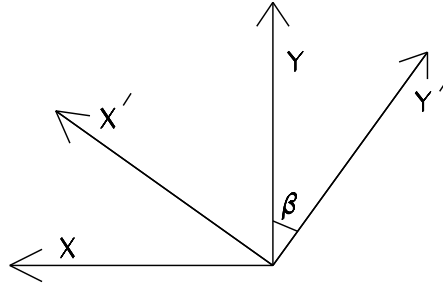


Figure 3: Axes x , y , x' and y' .

The relevance to galactic physics is that Fig. 1(a) includes mixing between Newtonian gravity (to the left of the figure) and the Hubble acceleration (to the right). In order to reproduce the symmetric form of Fig. 2, the Bogoliubov transformation is needed. It rotates Fig. 1(a) by 35.78° anti-clockwise; this is the mean angle of the dashed and dotted lines with respect to the x -axis. The rotation is illustrated in Fig. 3; it is about the point $x = -10$, $y = -10$, where the two straight lines of Fig. 1(a) cross:

$$x' = (x + 10) \cos \beta - (y + 10) \sin \beta \quad (20)$$

$$y' = (x + 10) \sin \beta + (y + 10) \cos \beta. \quad (21)$$

Substituting Eq. (10) gives an exact expression for the curve in x', y' axes.

It is also convenient to re-express g_N and the Newtonian energy directly in terms of x ; from Fig. 1(a)

$$H_{11} = E_1 = -GM/r = -\sqrt{GM}\epsilon^{x/2} \quad (22)$$

$$H_{22} = E_2 = \sqrt{GM}\epsilon(x) \quad (23)$$

$$V = \sqrt{GM}W(x'), \quad (24)$$

where ϵ refers to an energy possibly given by the Hubble acceleration; however, in practice, the effect of the Hubble acceleration over the radius of the Milky Way is $< 2 \times 10^{-4}$, which can be neglected. Note that the factor \sqrt{GM} appears in all three equations, so as to conform with Milgrom's scaling law. The common approximation is also used that the gravitational energy of a disc galaxy is $-GM/r$, where M is the mass inside radius r . This is accurate to $\leq 1\%$ at the large values of r of interest. The two solutions of the Breit-Rabi equation are

$$E = \frac{E_1 + E_2}{2} \pm \sqrt{\left(\frac{E_1 - E_2}{2}\right)^2 + V^2}. \quad (25)$$

3 The relation to a Fermi function

The acceleration differs in x and x' axes, but the scalar quantity W is independent of axes. The standard form of the Fermi function is

$$W(x) \propto \left[1 + \exp\left(\frac{E - E_F}{\beta E_F}\right) \right]^{-1}, \quad (26)$$

where E_F is the energy at the centre of the Fermi function and β is a fitted constant. This refers to a situation where there is a discrete energy gap, e.g. in a perfect semi-conductor or superconductor. $W(x)$ can be obtained by numerical integration of y from Eq. (10) and is shown as the full curve in Fig. 1(c).

3.1 A long-range logarithmic tail to the Newtonian potential

If there were no quantum mechanical mixing between Newtonian acceleration and the condensation mechanism, there would be no structure at the crossing point and, more serious, no explanation for the term $\sqrt{a_0 g_N}$.

Asymptotically, the total acceleration, taken from MOND, is

$$a = a_0 \sqrt{g_N/a_0}. \quad (27)$$

Since $g_N = GM/r^2$,

$$a \rightarrow \sqrt{GMa_0}/r. \quad (28)$$

Taking this as $-d\phi/dr$, where ϕ is a potential induced by the mixing,

$$\phi \rightarrow -\sqrt{GMa_0} \ln(r/r_1). \quad (29)$$

Here r_1 is the mean radius for this term. The value of r_1 is necessarily very close to the much larger dip caused by dW/dx . Because $a_0 \sim 10^{-10}$, ϕ is very small. However, it does explain the asymptotic straight-line at the right-hand edge of Fig. 1(a) and contributes to $\epsilon(x)$ in H_{22} .

The interpretation of this term is that mixing between the Newtonian potential and the condensation mechanism expands the wave-length of gravitons trapped in the Newtonian potential and lowers their zero-point energy. An analogy is the covalent bond in chemistry. In the hydrogen molecule, each of two electrons is attracted to two protons (which themselves repel one another). This increases the wave-length of the electrons and reduces their zero-point energy.

Sobouti noticed this long-range logarithmic component and wrote two closely related papers [25], [26]. These included effects of General Relativity. This is interesting but not strictly necessary at present. The problem was solved by Sobouti as a power series with additional empirical terms proportional to $1/r$ and $1/r^2$. These terms are now replaced by our equations. There is experimental evidence that the Milky Way has a halo extending to ~ 100 kpc [27]. However, this could be due to gas and dust shared with the local cluster of galaxies. So this halo is presently ambiguous.

3.2 Solving the Breit-Rabi equation

The binding energy W is defined with the same sign as E_1 . From equations (25) and (24),

$$2E = E_1 + \epsilon(x) \pm \sqrt{(E_1 - \epsilon(x))^2 + 4V^2} \quad (30)$$

$$= \frac{\sqrt{GM}}{\ln_{10}} \left(-e^{x/2} + \epsilon(x) \pm \sqrt{(e^{x/2} - \epsilon(x))^2 + 4W^2} \right) \quad (31)$$

$$2\frac{dE}{dx} = \frac{\sqrt{GM}}{\ln_{10}} \left(-0.5e^{x/2} + d\epsilon/dx \pm \frac{(e^{x/2} - \epsilon(x))(0.5e^{x/2} - d\epsilon/dx) + 4WdW/dx}{\sqrt{(e^{x/2} - \epsilon(x))^2 + 4W^2}} \right) \quad (32)$$

The factor \ln_{10} allows for the fact that Fig. 1(a) has been drawn using axes which use logarithms to the base 10. For the upper branch of the solution, the minus sign for the term involving the square root is required to reproduce the usual Newtonian potential. The equations simplify considerably if the very small term $\epsilon(x)$ is neglected.

A Bose-Einstein condensate does not fit the data. In this case, dW/dx should vary as $T^{3/2}$ at the peak of the acceleration [28]. For positive x near $x = 0$, the relation of the energy function to kT gives,

$$W(x) = -B(1 + |x|^{3/2} \exp -\gamma' x^2) \quad (33)$$

$$dW(x)/dx' = B(1.5|x|^{0.5} - 2\gamma'|x|^{5/2}) \exp -\gamma' x^2; \quad (34)$$

for negative x , the opposite sign of $|x|$ is needed in $W(x)$. The second term in $dW(x)/dx$ wrecks the x dependence, which fails to fit the observed peak. Near $x = 0$ it has a square root variation with x and then, when the second term of Eq. (34) overtakes it, the curve turns downwards. This rules out a Bose-Einstein condensate.

The depth of the Fermi function is $-0.5GM$. The magnitude of this term can be traced to the factor 2 difference in slope of g_N and that of the asymptotic form $\sqrt{a_0 g_N}$.

Let us now return to Figs. 1(b) and (c). Here there is a slight complication. Fig. 1(b) is the acceleration measured in x, y axes. However, the rotation to x', y' axes requires that γ of

Eq. (16) is increased to 1.852. In addition, there is a small visible displacement of the centre of curvature in Fig. 1(a) by an offset of -0.203×10^{-10} in x . What then emerges from the Breit-Rabi equation is that g_N is rather small near $x = a_0$ compared with that originating from the extra acceleration dW/dx' . This second term dominates by a large factor ~ 171 at the centre of the curve. This ratio falls by 50% at $x = -10.6$, to 30 at $x = -11$, then -6.0 at $x = -11.5$ and ~ 1 at $x = -12$. Results for the ‘extra’ acceleration are symmetric about a_0 except for the term $\sqrt{a_0 g_N}$ of Eq. (10). The conclusion is that the curved part of Fig. 1(a) is the dominant feature near $x = a_0$ where Newtonian gravitation is a rather small perturbation.

Consider the effect of this result near the centre of the Fermi function at $E = E_F$ in Fig. 1(c). If we retain only the dominant terms in W and dW/dx , Eqs. (31) and (32) give

$$dE/dx \rightarrow \frac{\sqrt{GM}}{\ln_e 10} 2dW/dx \quad (35)$$

$$E \rightarrow \frac{\sqrt{GM}}{\ln_e 10} 2W. \quad (36)$$

Apart from the factor $\sqrt{GM}/\ln_e 10$, which is a normalisation factor, dE/dx may be interpreted as the modulus of a Breit-Wigner resonance with x -dependent width:

$$BW = \frac{\Gamma(x)/2}{E - E_F - i\Gamma(x)/2}. \quad (37)$$

The energy W starts at zero because of local gauge invariance, and its central value is shifted downward by 0.25 GM. This accounts for the form of Eq. (8) of Section 2, where two terms $(a_0/2a)^2$ cancel.

How can this effect be understood? A possibility is that the graviton acquires a small effective mass near a_0 . The fitted change to the gravitational acceleration is close to a Gaussian, as in Fig. 1(b). In subsection 2.1, the dependence of the fit on alternative forms of Milgrom’s μ function was tested. Although acceleration curves change significantly, the Fermi function is affected only at the ends of the range $x = 8$ to 12 by at most $\pm 4\%$.

The conclusion from these results is that the central part of the Fermi function is stable, but can be perturbed at the edges. In superconductors, a coherence length was introduced by Pippard to account for the effects of defects beyond an experimentally observed range [29]. It appears that galaxies behave similarly. If gravitons acquire an effective mass, it appears at first sight that this will weaken gravity. However, remember that the wave-lengths of gravitons on a galactic scale are very large. The spectrum of gravitons near the edge of the galaxy is a convolution of gravitons from the rest of the galaxy. Gravitons from the galactic centre become almost plane waves which can interact coherently over a large volume. They function like phonons coupling to Cooper pairs in a superconductor producing an energy gap. A coherence length like that introduced by Pippard can arise in many ways. Supernovae act as major perturbations, heating sizable volumes. It is also known that so-called chimneys and wormholes provide channels through which currents of dust and gas flow. Furthermore, one of the remarkable features of galaxies is that they only grow to a certain size. The largest have masses of order $10^{12} M_\odot$. This can be attributed to the rapid fall-off of the ‘extra’ acceleration due to MOND close to $x = -8$ and -12 . All of these effects point to a coherence length due to the variation of the Fermi function in Fig. 1(c).

Let us return to a simpler issue, the missing lower branch of the Breit-Rabi equation. On this branch both W and dW/dx' change sign. The change of sign requires that this branch describes an excited state rather than a condensate. (Remember that energies of both gravity and $W(x)$ are negative). Such an excited state is likely to decay on a time scale much less than that of galaxies, so it is unlikely that this branch will be observable. For those wishing to investigate this branch, the procedure is (a) to fit the upper branch as a function of x , (b) rotate to x', y' axes, (c) reverse the sign of y' to reach the lower branch, and (d) rotate axes back again to x, y . The best place to search for this branch is near the crossing point of Fig. 1(a).

4 The relation to Dark Energy

Experiment tells us that in galaxies, the asymptotic form of the acceleration is $\sqrt{a_0 g_N}$. This leads to the question: what governs the asymptotic acceleration?

If MOND successfully models the formation of galaxies and globular clusters, it raises the question of how to interpret Dark Energy. In a de Sitter universe, the Friedmann-Robertson-Walker model smoothes out structures using a Λ CDM function which models the gross features. These change over the lifetime of the Universe. However, if quantum mechanics governs individual galaxies, there will instead be fine structure in Dark Energy. It is logical that steps like Figs. 1(c) do not just average out, but instead accumulate over all of this fine structure.

The standard treatment of Dark Energy is reviewed by Sami [30]. The acceleration falls initially due to Newtonian cosmology. However, at recent times, the acceleration increases. This acceleration can be explained naturally by the sum total of the fine structure over all the galaxies. The total acceleration is parametrised via the assumed time dependence of the metric on the Hubble acceleration. A similar suggestion along these lines has been advanced by Zhang and Li [31] using ideas based on entropic arguments. The ‘present-day’ Hubble acceleration is the local value and varies over the Universe according to the parametrisation by Dark Energy.

There is a further argument pointing towards the idea that local fine structure is cumulative. Peebles and Nusser argue that galaxies condense more rapidly than the standard Λ CDM model predicts [32]. In particular, they point out that the Local Void contains far fewer galaxies than Λ CDM predicts statistically, while there is an unexpected presence of large galaxies on the outskirts of the Local Void. Their Fig. 1 is very persuasive in this respect. Only 3 galaxies are observed in the Local Void compared with 19 predicted. The Poisson probability for this result is of the order 10^{-5} from Λ CDM. Peebles and Nusser conclude: ‘In short, the general sensitivity of galaxies to their environment is not expected in standard ideas. It would help if galaxies were more rapidly assembled so that they could then evolve as more nearly isolated island universes.’ Later Peebles considered an additional empirical term added to the Λ CDM model, but commented that the change requires that Cold Dark Matter is cored rather than the expected cusped behaviour [33].

A natural explanation is that the Local Void gives no contribution to the Hubble mechanism, except for its three galaxies. The total energy E is then higher there. On the periphery of the Void, there is gas and dust which can form galaxies. This gas runs down the energy gap to enlarge galaxies forming there. Galaxies then grow by accumulation of dust and gas. The condensate at the edge of the galaxy acts as a funnel to collect gas and dust. Towards the centres of galaxies, they can develop in different ways depending on the angular momentum

L of the galaxy. For large L , they naturally form flat discs. For lower L , bulges develop and spiral arms; these features can vary according to whether the galaxy is supported by rotation or pressure or both. For really low L , large elliptical galaxies and dwarf spherical galaxies develop. If L is close to 0, galaxies collapse as quasars. It appears that Λ CDM is presently fitting all these different morphologies with a very flexible ansatz for Dark Matter.

So far, Dark Matter has escaped experimental detection. There are speculations that it may take the form of sterile neutrinos with masses in the electron-volt range. At a recent conference on neutrino physics, Altarelli commented on this question [34]. He argued that more than one sterile neutrino is disfavoured by stringent bounds arising from nucleosynthesis. Also there is tension between LSND, MiniBoone and KARMEN experiments leaving little room for a signal. Rubbia et al. propose a new neutrino detector ICARUS-NESSIE to run at CERN with parameters optimised for finding sterile neutrinos [35].

There is also speculation about Grand Unified Theories in which massive right-handed neutrinos couple weakly to left-handed light neutrinos. Such heavy neutrinos would have formed in the Big Bang before the generation of the Cosmic Microwave Background. If these heavy neutrinos survive and mix with light neutrinos, their lifetimes must be larger than the age of the Universe, otherwise there would be effects visible in Dark Energy.

4.1 Other Condensates

Well known examples of condensates are ferromagnets and anti-ferromagnets. In ferromagnets, spins align parallel with one another below the Curie point; in the absence of a magnetic field, the overall spin can lie in any direction. In anti-ferromagnets they spontaneously align anti-parallel. The ground-states of these systems have a lower symmetry than the Hamiltonian. This is a purely quantum effect, but difficult to calculate from first principles. However, neutron scattering experiments establish the structures. In astrophysics, the situation is difficult because one can only watch how galaxies evolve.

In Particle Physics, we now know that the Strong Interaction is mediated by massless gluons obeying Chiral Symmetry, i.e. they do not discriminate between left-hands and right-hands. Below a mass of ~ 1 GeV, the gluon acquires an effective mass from its interaction with light quarks, which themselves have masses of ~ 4 and 9 MeV. The Electroweak Theory is constructed from a mixing between Electromagnetism and Weak Interactions carried by W and Z particles and probably the Higgs boson. A side-effect of this idea is that Chiral Symmetry is broken in the strong interactions for spin 0 particles below 1 GeV. This idea was introduced by Gasser and Leutwyler [36] and today gives many quantitatively accurate results in meson spectroscopy. An important step in understanding the precise mechanism was made by Bicudo and Ribiero [37]. Their work finds the Bogoliubov-Valatin transformation to be an essential element. Above 1 GeV, there is a cross-over in which Chiral Symmetry is largely restored and the quark model reigns supreme, though with small amounts of mixing with meson-meson and/or $q\bar{q}q\bar{q}$ basis states. A recent paper of Pennington and Wilson gives details including figures showing the cross-over at 1 GeV [38].

A precise set of equations describing Chiral Symmetry Breaking is given by Cherney et al. [39]. This work shows that gauge invariance requires that quarks must be treated as ‘dressed’ fermions, rather than bare fermions. Their conclusion is that a Yukawa potential appears explicitly in the $q\bar{q}$ interaction, their Eq. (61). This increases the fermion mass from a few MeV to the so-called

constituent mass, ~ 320 MeV. In their Eq. (72), a logarithmic term appears from Feynman diagrams where one pair of particles rescatter to themselves through a closed loop. The origin of Chiral Symmetry Breaking is that quarks have small masses; if these were zero, the pion would be massless.

In summary, it is clear that there are three gauge fields: (i) gluons, (ii) electromagnetism linked to weak interactions, and (iii) gravity. Effective masses do arise in the first two. There has been a paper by Van Dam and Veltman [40] claiming a no-go theorem preventing the graviton developing a mass. This theorem appears to refer purely to an isolated graviton obeying General Relativity. That is different to the present case where the condensate is a property of the graviton-nucleon interaction.

There is an important point if gravitons develop an effective mass. In Particle Physics, there are relations between scattering processes such as $\pi^+p \rightarrow \pi^+p$, $\pi^-p \rightarrow \pi^-p$ and $\pi^+\pi^- \rightarrow p\bar{p}$. Amplitudes depend on $E^2 - p^2$, where E and p are momenta in each reaction. These are denoted s , u and t -channels by a convention introduced by Mandelstam. For massless gravitons, kinematics of the s -, t - and u - channels all meet at a point. However, if the graviton acquires an effective mass, it moves these three channels apart and changes the graviton-nucleon interaction. In particular, it affects the nucleon pole term in the u -channel, hence the structure of the nucleon. What is needed, but beyond reach at present, is to solve the Schwinger-Dyson equations for this case following the procedure of Pennington and Wilson for the $\pi\pi$ system. The obstacle is that the structure of the nucleon is not yet known precisely enough for a realistic calculation from first principles. Thomas developed a model in 1983 explaining features of deep inelastic scattering (i.e. large momentum and energy transfers in electron scattering from nucleons) which provided a qualitative explanation of the data in terms of a chiral quark model [41]. The idea is that a nucleon has a component in its wave function with a pion circulating round it with one unit of orbital angular momentum: $N \rightarrow [N + \pi]_{L=1}$. This has been followed up in a recent paper of Burkhardt et al. which improves this work in specific ways [42], but the final set of parameters is not yet available.

Cosmology needs to be treated equally empirically. My suggestion is that Dark Energy is symptomatic of spontaneous symmetry breaking of gravitation to a de Sitter universe governed by the space and time components of the metric. The de Sitter universe has a lower symmetry than General Relativity. In galaxies, a_0 is the order parameter of a Fermi-Dirac condensate and is directly related to $cH_0/2\pi$. The origin of the factor 2π is the same as that between Planck's constant and \hbar . In both cases, what is involved is a transformation from spherical or cylindrical coordinates to Cartesian coordinates.

5 Further work which is needed

The model proposed here is precise and open to experimental test. The most important and simplest is that if Dark Matter is replaced by this model, it is obviously necessary to redo the parametrisation of Dark Energy so that it reproduces smoothly what has been parametrised as Dark Matter up to now. This does not necessarily require major modifications. The main point is to fit the third peak in the Cosmic Microwave Background. This requires cooperation of groups with the latest Planck data and techniques at their finger-tips. Despite the clues pointed out here that a Fermi-Dirac condensate explains galactic rotation curves, this could fail. It

would not be surprising if minor modifications are required in the refit to Dark Energy and new clues might emerge. It is necessary to include the logarithmic tail of the Newtonian potential found here. It is also essential to treat Voids so that they only contribute to Dark Energy via the galaxies observed there. Those may not be well resolved if they are very distant from us. It is also essential to fit the Hubble parameter and magnitudes of Type1a supernovae as a function of red-shift z .

Whatever develops at the edges of galaxies will affect both Strong and Weak Gravitational Lensing. However, unless data are used where a distant quasar transmits light through the periphery of a galaxy, where the effect of $W(x)$ is large, the lensing effect will be rather small. The weak logarithmic tail of Newtonian gravitation also needs to be taken into account.

What happens in clusters of galaxies needs detailed, laborious calculations using the formulae given here; since there are presently claims that Milgrom's formula does not correctly reproduce what happens in clusters, this could be revealing. A multi-body interaction between the Hubble mechanism and several galaxies is required. Quite apart from the attraction to acceleration a_0 , there are also strong tidal effects of the variety discussed by Kroupa [43].

The same remarks apply to the Bullet Cluster, which needs to be refitted with the model proposed here. The calculation becomes a two-centre problem. The Hubble acceleration couples to both galaxies, but they also couple to one another, modifying the zero-point energy; individual stars in galaxies communicate with one another not only through the Newtonian potential but via their Fermi functions. In the Bullet Cluster, each galaxy behaves in this way, but there will be coupling between stars "belonging" to each individual galaxy. There may be complex interactions between the two galaxies including resonance effects. There are new data on the Bullet Cluster [44] showing that there are many dwarf satellite galaxies in the cluster.

6 Concluding Remarks

The equations given here allow very little freedom - just the 4% perturbations allowed in the Fermi function at the top and bottom of Fig. 1(c). There are five clues which point to galaxies and globular clusters being quantum mechanical condensates.

1. The phenomena of Fig. 1 appear on a logarithmic scale of g_N . This is the form expected for the Partition function of Statistical Mechanics:

$$Z = \Pi_s \frac{1}{1 + e^{E_s/kT}} \quad (38)$$

where E_s are energies of levels in a box and Π denotes the numbers of quantum levels in the box. For a refresher course, see Schrödinger's clear exposition [45].

2. Fig. 1(a) can be interpreted in terms of quantum mechanical mixing between two crossing eigenstates; the rotation of axes accommodated by Fig. 3 is just what is expected from the Bogoliubov-Valatin transformation, a quantum effect.
3. Fig. 1(c) is fitted naturally by a Fermi function with an energy gap $0.5 GM$.
4. The asymptotic form of the acceleration in Fig. 1(a) generates a logarithmic tail; this requires a quantum mechanical explanation. A Fermi-Dirac condensate fits the data; a Bose-Einstein condensate does not.

5. Long wave-length gravitons can explain the amplification of the amplitude forming the condensate.

The lower branch of the Breit-Rabi equation has the opposite curvature to the upper one. The natural interpretation of this result is that it corresponds to an excited state which will decay rapidly and will not therefore appear in galactic rotation curves.

The interpretation of the curve of Fig. 1(b) as an energy-dependent Breit-Wigner pole is that the graviton acquires an effective mass in the vicinity of a_0 . How this originates is speculative but does not reflect on the five clues listed above; it depends on the nucleon structure function which is not yet well defined.

The asymptotic form of the acceleration is $\sqrt{a_0 g}$. This is clearly associated with the Hubble acceleration and is related to Dark Energy. The standard approach to the Universe is the Friedmann-Robertson-Walker model where components of the metric are smoothed over local structures and appear in the radial and time components of the metric of General Relativity. My suggestion is that galaxies create fine-structure and the Friedmann-Robertson-Walker model should include into Dark Energy the sum over these structures. This may explain the agreement between a_0 and $cH_0/2\pi$ in our part of the Universe as well as its late-time acceleration.

Those are the essential points. They do reflect successfully the facts which MOND parametrises. However, only the peripheries of galaxies are considered. The morphology at the centres of galaxies is a separate issue.

There are two further small comments. Firstly, there have been many papers on the derivation of Newton's law from Entropic arguments. Many assume that one can assign a temperature T_0 to the Hubble acceleration and a temperature T_1 for the gravitational potential by adding them as the sum of squares, i.e. the random phase approximation. This gives the result for the total acceleration:

$$a = \sqrt{(g_N + g_H)^2 - g_H^2} \quad (39)$$

where g_H is the Hubble acceleration $H_0^2 r$, and r is the distance to the centre of the gravitating object. This is a quite different approach to the one proposed here and leads to a very small effect. For the Milky Way, it is a maximum of $2 \times 10^{-4} cH_0/2\pi$.

Secondly, Iorio has calculated that effects of MOND on the perihelia of planets in the Solar system are about a factor 10 below present experimental errors [46]. The logarithmic term arising from MOND will be of order a_0 , which is very small and will vary exceedingly slowly over the solar system. It has been pointed out by Galianni et al. that it may be feasible to detect the MOND effect at acceleration a_0 in the solar system near Lagrangian points where the accelerations of the Sun, Earth and Moon cancel out [47]. If measurements of sufficient accuracy could be made, they might confirm or modify MOND as a model of the behaviour of galaxies; secondly, they have the important potential to measure the shape of the response function through the region where the bend appears in Fig. 1. Further study of globular clusters would also provide information on the rotation curves of galaxies.

ACKNOWLEDGEMENT

I wish to thank Prof. Pedro Bicudo for discussions about Bose-Einstein condensates.

References

- [1] B. Famaey and S.S. McGough, arXiv: 1112.3960.
- [2] M. Milgrom, *Astrophys. J* **270** 371 (1983).
- [3] M. Milgrom, *Astrophys. J* **270** 384 (1983).
- [4] M. Milgrom, *ApJ* **698** 1630 (2009).
- [5] N.B. Tully and J.R. Fisher, *Astron. Astrophys.* **54** 661 (1977).
- [6] S.S. McGaugh, *Astrophys. J* **632** 859 (2005).
- [7] P. Kroupa, M. Pawlowski and M. Milgrom, arXiv: 1301.3907.
- [8] B. Famaey and S.S. McGough, arXiv: 1301.0623.
- [9] S. McGaugh and M. Milgrom, *Astrophys. J* **766** 22 (2013).
- [10] M.L.M. Collins *et al.*, arXiv: 1302.6590.
- [11] R.A. Ibata *et al.* arXiv: 1301.0446.
- [12] F. Lüghausen *et al.* arXiv: 1304.4931.
- [13] R. Scarpa *et al.*, *Astron. Astrophys.* **525** A148 (2011).
- [14] X. Hernandez and M.A. Jiménez, *Astrophys. J* **750** 9 (2012).
- [15] X. Hernandez, M.A. Jiménez and C. Allen, arXiv: 1206.5024.
- [16] M. Milgrom, *Proc. 2nd Int. Workshop on Dark Matter (DARK98)* eds. H.V.Klapdor-Kleingrothaus, L. Baudis: arXiv: astro-ph/9810302.
- [17] S.W. Hawking, *Comm. Math. Phys.* **43** 199 (1975).
- [18] N.N. Bogoliubov, *J. Exptl. Theor. Phys. (U.S.S.R)* **34** 58,73 (1958);
translation: *Soviet Phys. JETP* **34** 41, 51 .
- [19] J.G. Valatin, *Nu. Cim.* **7** 843 (1958).
- [20] M. Milgrom, arXiv: 0908.3842.
- [21] S.S. McGaugh, arXiv: 1107.2934.
- [22] G. Gentile, B. Famaey and W.J.G. de Blok, *Astron. Astrophys.* **527** A76 (2011).
- [23] D.V. Bugg, *J. Phys. G: Nucl. Part. Phys.* **35** 075005 (2008).
- [24] G. Breit and I.I. Rabi, *Phys. Rev.* **38** 2082 (1931).

- [25] Y. Sobouti, arXiv: 0812.4127.
- [26] Y. Sobouti, arXiv: 0810.2198.
- [27] A.J. Deason *et al.* arXiv: 1205.6203.
- [28] D.R. Tilley and J. Tilley, *Superfluidity and Superconductivity*, Adam Hilger, Bristol and New York, 3rd Edition (1990).
- [29] A.B. Pippard, Proc. R. Soc. A **216** 547 (1953).
- [30] M. Sami, Curr. Sci. **97** 887 (2009).
- [31] H. Zhang and X-Z Li, Phys. Lett. B **715** (2012) 15.
- [32] P.J.E. Peebles and A. Nusser, Nature **465** 565 (2010).
- [33] P.J.E. Peebles, arXiv: 1204.0485.
- [34] G. Altarelli, arXiv: 1304.5047.
- [35] C. Rubbia, A. Guglielmi, F. Pietropaolo, and P. Sala.
- [36] J. Gasser and H. Leutwyler, Phys. Lett. B **125** (1983); Annals Phys. **158** (1984) 142.
- [37] P. D. de A. Bicudo and J.E.F.T. Ribiero, Phys. Rev. D **42** 1611 (1990).
- [38] M.R. Pennington and D.J. Wilson, Phys. Rev. D **84** 094028 and 119901 (E).
- [39] A.Yu, Cherny, A.E. Dorokhov, Nquyen Suan Han, V.N. Pervushin and V.I. Pervuhin, arXiv: 1112.5856.
- [40] H. van Dam and M.J.G Veltman, Nucl. Phys. B **22** 397 (1970).
- [41] A.W. Thomas, Phys. Lett. B **126** 97 (1983).
- [42] M. Burkhardt, K.S. Hendricks, Chueng-Ryong Ji, W. Melnitchouk and A.W. Thomas, arXiv: 1211.0485.
- [43] P.Kroupa, arXiv: 1204.0485.
- [44] D. Paraficz *et al.* arXiv: 1209.0384.
- [45] E. Schrödinger, *Statistical Thermodynamics*, Cambridge University Press, 2nd Edition (1952).
- [46] L. Iorio, arXiv: 0905.4704.
- [47] P. Galianni, M. Feix, H.S. Zhao and K. Horne, arXiv: 1111.6681.